Published online 9 July 2018

Nucleic Acids Research, 2018, Vol. 46, No. 17 ***8803–8816***
doi: 10.1093/nar/gky584

The conserved regulatory RNA RsaE down-regulates the arginine degradation pathway in *Staphylococcus aureus*

Tatiana Rochat[1,2], Chantal Bohn[1], Claire Morvan[1], Thao Nguyen Le Lam[1], Fareha Razvi[3], Adrien Pain[1], Claire Toffano-Nioche[1], Prishila Ponien[4], Annick Jacq[1], Eric Jacquet[4], Paul D. Fey[3], Daniel Gautheret[1] and Philippe Bouloc[1,*]

[1]Institute for Integrative Biology of the Cell (I2BC), CEA, CNRS, Université Paris-Sud, Université Paris-Saclay, 91190 Gif sur Yvette, France, [2]VIM, INRA, Université Paris-Saclay, 78350 Jouy-en-Josas, France, [3]University of Nebraska Medical Center, Department of Pathology and Microbiology, Omaha, NE, USA and [4]Institut de Chimie des Substances Naturelles, CNRS UPR 2301, Université Paris-Sud, Université Paris-Saclay, 91190 Gif sur Yvette, France

Received November 04, 2017; Revised May 28, 2018; Editorial Decision June 14, 2018; Accepted June 29, 2018

ABSTRACT

RsaE is a regulatory RNA highly conserved amongst Firmicutes that lowers the amount of mRNAs associated with the TCA cycle and folate metabolism. A search for new RsaE targets in *Staphylococcus aureus* revealed that in addition to previously described substrates, RsaE down-regulates several genes associated with arginine catabolism. In particular, RsaE targets the arginase *rocF* mRNA *via* direct interactions involving G-rich motifs. Two duplicated C-rich motifs of RsaE can independently downregulate *rocF* expression. The faster growth rate of Δ*rsaE* compared to its parental strain in media containing amino acids as sole carbon source points to an underlying role for RsaE in amino acid catabolism. Collectively, the data support a model in which RsaE acts as a global regulator of functions associated with metabolic adaptation.

INTRODUCTION

Staphylococcus aureus is a major human opportunistic pathogen that is responsible for diseases ranging from minor skin infections to life-threatening septicemia and toxic shock syndrome. Its virulence is associated with its ability to survive in different ecological niches and to coordinate the expression of virulence factors. Two alternative sigma factors, σ^B and σ^S, contribute to adaptation (1,2), with σ^B modulating the expression of numerous virulence factors and is required for long-term persistence *in vivo* (3). The expression of virulence genes is affected by energy resources and the use of carbon sources is tightly regulated by global regulators such as CcpA and CodY (4–6). Numerous *trans*-acting regulators, including regulatory RNAs (sRNAs), contribute to this adaptation (7,8).

sRNAs are highly abundant in bacteria (9,10). Many of them modulate mRNA translation and stability by base-pairing with one or several targeted RNAs. They act on almost all cellular functions, contributing to adaptation and bacterial homeostasis (11). In *S. aureus*, the functions and targets of most sRNAs are unknown. RNAIII is one exception; this 514-nucleotide (nt) sRNA has been extensively studied and is a paradigm for regulatory RNAs affecting virulence (12). A second 102-nt sRNA, RsaE, drew the attention of researchers because of its high conservation in the *Bacillales* order (13). In *Bacillus subtilis*, the RsaE homolog RoxS downregulates transcripts associated with redox reactions, contributing to the cellular NAD^+/NADH balance (14,15). In *S. aureus*, RsaE affects the expression of several genes involved in oligopeptide transport, folate metabolism and the TCA cycle (16,17). *In vitro* experiments on some targets suggested that RsaE and RoxS bind mRNA Shine-Dalgarno (SD) sequences to prevent the formation of ribosomal initiation complexes (14,16,17). A C-rich motif, repeated in RsaE, and present in other staphylococcal sRNAs, reportedly contributes to an RNA-RNA pairing mechanism that is common to different sRNAs (17). These duplex formations generate RNase III cleavage sites that irreversibly prevent translation (7,14). In contrast to numerous Gram-negative bacteria, in *B. subtilis* and *Staphylococcus aureus*, the RNA chaperone Hfq is likely not required for sRNA-dependent regulations (18–20).

rsaE transcription is induced in mid- or late-exponential phase as observed in various strains. Its expression is significantly reduced post-exponentially in strain N315 and clinical isolates (16,17,21). *rsaE* is regulated by the two-

*To whom correspondence should be addressed. Tel: +33 1 6982 6217; Email: philippe.bouloc@cnrs.fr
Present address: Adrien Pain, Bioinformatics and Biostatistics Hub (C3BI), USR 3756 IP CNRS, Institut Pasteur, Paris, France.

component system SrrAB (14), which is likely activated in response to reduced menaquinone (22).

Here, by combining different approaches and selecting common candidates, we identified new targets of RsaE. We investigated RsaE mechanism of action and demonstrated that it exerts direct post-transcriptional regulation on a gene associated with arginine catabolism. Growth analysis in media containing amino acids as the only carbon source further reveals that the absence of RsaE results in enhanced growth rate, which is consistent with the up-regulation of associated catabolic pathways.

MATERIALS AND METHODS

Bacterial strains, plasmids and growth conditions

This study was performed using HG003, a model strain for *S. aureus* regulation (23), and constructed derivatives (Supplementary Table S1). For HG003 gene description, the NCTC8325 nomenclature retrieved from Genbank file CP00025.1 was used. Engineered plasmids were constructed in *Escherichia coli* DH5α, transferred to RN4220 (a strain transformable by exogenous DNA) and subsequently to HG003. Chromosomal gene modifications (deletions and point mutations) were performed using pMAD2 derivatives as described (24). Conditional gene expression was obtained by cloning genes under the *xyl*/*tetO* promoter in pRMC2 (25). Translational regulations were studied by gene fusions with untranslated transcriptional regions (UTRs) + the first codons cloned downstream the *rpoB* promoter as reported (26) using pTCV-PrpoB-*lac* (Supplementary Table S2), a pTCV-*lac* derivative (27). Plasmids (Supplementary Table S2) were engineered mainly by the Gibson assembly method (28) with the indicated appropriate primers (Supplementary Table S3).

Staphylococcus aureus strains were routinely grown aerobically in Brain Heart Infusion (BHI) broth at 37°C. DH5α was grown aerobically in Luria-Bertani (LB) broth at 37°C. Antibiotics were added to media as needed: ampicillin 100 μg/mL, chloramphenicol 20 μg/ml for *E. coli*; chloramphenicol 10 μg/ml and erythromycin 5 μg/ml for RN4220; chloramphenicol 5 μg/ml and erythromycin 0.5 μg/ml for HG003. Expression of *rsaE* and mutated *rsaE* under the control of promoter $P_{xyl/tetO}$ (pRMC2RsaE and mutated derivatives) was induced by the addition of anhydrotetracycline (aTc, 1 μM) to culture medium.

Growth in complete defined medium (CDM) and metabolite analyses

S. aureus HG003 and HG003 Δ*rsaE* were grown aerobically (250 rpm and 10:1 flask-to- volume ratio) in CDM lacking glucose as previously described (29,30). The CDM contains 18 amino acids excluding glutamine and asparagine. For amino acid analysis, 1 ml of bacterial culture was collected during growth and centrifuged at 14 000 g to collect supernatant. Supernatant was subsequently filtered through an Amicon Ultra Centrifugal filter (Amicon; 3000 molecular weight cut off). Amino acid concentration was determined using a Hitachi L-8800 amino acid analyzer at the University of Nebraska Medical Center Protein Structure Core Facility. Statistical analyses were performed using PC SAS version 9.4. The statistical level of significance was set to 0.05 for all analyses. For each amino acid, a general linear model was fit that included a term for group (Δ*rsaE* versus wild-type) and the continuous covariate OD. Residuals from the model were tested for normality using the Wilks-Shapiro test.

Total RNA extraction

Overnight cultures were diluted 1000 times and incubated in BHI at 37°C. For HG003 and HG003 Δ*rsaE*, bacteria were harvested at OD_{600} of 6. For HG003 Δ*rsaE* pRMC2RsaE, at OD_{600} of 0.5, the culture was split in two halves and aTc (1 μM) was added to one of them for *rsaE* induction. Induced and non-induced cultures were harvested 5 min after aTc addition. Total RNAs were extracted as described (19). Samples were prepared in triplicates and treated with TURBO DNase (Ambion) according to manufacturer's instructions. Ten microgram of RNA were processed using MICROBExpress (Ambion) according to manufacturer's instructions to remove ribosomal RNA. RNA-seq libraries were generated with the TruSeq SBS Kit v3 (Illumina) and sequenced using a HiSeq to generate paired-end 100-nt reads.

Hybrid-trap-seq

The procedure is summarized in Supplementary Figure S1. Synthetic RNAs were generated with the T7 MEGAshortscript kit (Ambion) according to manufacturer's instructions, using sRNA genes that were PCR-amplified with specific oligonucleotides (Supplementary Table S3). Synthetic RNAs were 3′-end biotinylated as described (31) using biotinamidocaproyl hydrazide (Sigma-Aldrich, B3770). After the biotinylation reaction, full length RNAs were purified on 5% urea PAGE as recommended in the T7 MEGAshortscript kit procedure. Running Hybrid-trap-seq requires a pool of total RNA extracts to be used as prey. Total RNA samples were extracted in 16 different biological conditions (referred to as 16-condition RNA pool): (i) eight samples grown in BHI at OD_{600} of 0.6, 1.8, 3.3, 4.5, 7.2, 9.8 and 12.8, and late stationary phase (24 h), (ii) seven samples grown under stress conditions (cold shock, heat shock, oxygen limitation, alkaline stress, peroxide stress, disulfide stress, iron-depletion) and (iii) one sample from colonies on BHI-agar plates. The complete description of the 16-condition RNA pool is available in the GEO database (GEO accession number: GSE104971) (10). Twenty μg of each of the 16 total RNA extracts were pooled to obtain the combined RNA extract sample used for the procedure. Hybrid-trap-seq experiments were then carried out as follows: MasterBeads precoated with streptavidin (Ademtech, Pessac-France) were equilibrated in binding buffer (20 mM Tris–HCl, 0.5 M NaCl pH 8) and incubated 10 min at 20°C with 100 pmol of biotinylated sRNA. Unbound sRNAs were removed by magnetic separation, and then sRNA-bound streptavidin beads were washed twice with binding buffer. Fifty μg of 16-condition RNA pool were mixed with the sRNA-bound beads. After 15 min at 45°C, followed by 15 min at room temperature, unbound RNAs were removed by magnetic separation. The RNA-bound beads were washed twice with

wash buffer (7 mM Tris–HCl pH 8, NaCl 0.17 M). RNAs were then eluted in RNase-free water. RNA samples were analyzed by Illumina high throughput sequencing. Five oriented libraries were generated from the four Hybrid-trap eluted RNA samples and the 16-condition RNA pool depleted of rRNA used as prey, as described (32). Libraries were sequenced using Illumina Genome Analyzer IIx to generate single-end 40-nt reads, which were then analyzed.

Read mapping and differential expression analysis

Quality control of all transcriptome samples using FastQC (v0.10.1) confirmed that the reads could be directly used for the mapping step. Reads were aligned to the *S. aureus* NCTC8325 chromosome sequence (CP000253.1) using bowtie2 mapper (v2.1.0) and default values (33). Log-read coverage profiles were computed using in-house shell scripts as described (32) and visualized in the Artemis viewer (34). Uniquely mapped read counts per gene were calculated for each dataset with feature Counts (1.5.0-p1, with options specifying paired-end and stranded library) (35) using the list of CDS retrieved from Refseq CP000253.1. The list of CDSs differentially expressed between two conditions (i.e. Δ*rsaE* mutant *versus* wild-type strain; induced *versus* non-induced RsaE expression) was supplied by SARTools v1.3.0 (36) using DESeq2 (37), with a false discovery rate (FDR) set at 0.05. Genes with a fold change >1.33 were considered as differentially expressed. Due to an outlier library identified by PCA and *P*-value analysis in the wild-type versus Δ*rsaE* mutant comparison, differential analysis of these conditions was performed using only replicates 1 and 3 and corrected for batch effect between pairs of replicates. The differential expression analysis between with and without induction of the RsaE expression was done with the three replicates. To identify RNAs specifically enriched with RsaE as sRNA-bait, Hybrid-trap-seq samples were analyzed as follow. Mapping was performed on the list of CDS retrieved from Refseq CP000253.1 and the 44 HG003 *bona fide* sRNA list recently established (10) using bowtie with parameters -p 12 -S -m 1 –q. Read counts per gene were then calculated with HTSeq-count (http://htseq.readthedocs.io/). Raw read counts of the four datasets (namely, RsaE, RsaA, RsaH and RNAIII used as bait) were normalized using DESeq and fold changes were computed from normalized read counts of RsaE-bait dataset to normalized read counts of control datasets (i.e. the three other sRNA datasets). Genes considered as putative sRNA targets displayed fold changes ≥10.

Computational analysis of RNA-RNA hybrids

Target RNA-sRNA interactions were predicted using the IntaRNA package (38); scoring is based on hybridization free energy and accessibility of the interaction sites in both RNA molecules (IntaRNA V 2.1.0 through the web interface at http://rna.informatik.uni-freiburg.de with default parameters). For Figure 2, complete sRNA sequences were used as input, and each putative target comprised the region from the transcriptional start site (TSS) to 150 nucleotides past the start codon. When possible, TSSs were defined from sequencing of the 16-condition RNA pool as described (32). Coordinates of relevant transcripts are provided (Supplementary Table S4). We searched for consensus motifs in the twelve putative target sequences and *rsaE* (in antisense) using the MEME suite V.4.9.0 (39) run locally with options -dna -minw 4 -maxw 10. Input sequence fragments were from TSS to ATG+150. The standard SD motif was identified by MEME using as input the 1114 *S. aureus* sequences for which a TSS could be identified by the above protocol.

Quantitative reverse transcriptase PCR and northern blots

qRT–PCR experiments were performed on a subset of putative targets selected among the most enriched mRNAs of RsaE Hybrid-trap-seq set. Experiments were performed on biological triplicates and data were analyzed as described; the geometric mean of 4 genes (*recA*, *gyrA, glyA* and *ftsZ*) was used to normalize the samples (40). All Northern blots were performed as described in duplicates (41–43). Samples were separated by either PAGE or agarose gels and probed with ^{32}P-labeled PCR probes using the Megaprime DNA labeling system (GE Healthcare) (for primer used, see Supplementary Table S3).

β-Galactosidase assay

The effect of RsaE on translation was tested by means of gene fusions with *lacZ* (pTCV-PrpoB-1138-lac and pTCV-PrpoB-rocD-lac) by β-galactosidase assays with two experimental settings: by comparing i) the Δ*rsaE* and its parental strains and ii) the Δ*rsaE* strain carrying pRMC2RsaE with and without RsaE induction. Overnight cultures grown in BHI supplemented with chloramphenicol and kanamycin (when necessary) were diluted 1000-fold in the same medium at 37°C. Δ*rsaE* and its parental strain were sampled at OD_{600} ∼7. For Δ*rsaE* carrying pRMC2RsaE, aTc (1 μM) was added to the medium at OD_{600} ∼0.5; cultures were sampled after a 15 min induction and frozen. β-galactosidase activity was measured with MUG (4-methylumbelliferyl beta-D-galactopyranoside, Sigma-Aldrich) as described (44). Briefly, cell pellets were resuspended in 500 μl ABT buffer (100 mM NaCl, 60 mM K_2HPO_4, 40 mM KH_2PO_4, 0.1% triton X100) and 10 mg/ml MUG. After 1 h incubation at 25°C, the reaction was stopped by addition of 500 μl Na_2CO_3 0.4 M. OD_{600} and fluorescence (excitation: 365 nm; emission: 455 nm) were measured with CLARIOStar (Monochromator Microplate Reader). The fluorescence of each sample was normalized by its OD_{600}. Translation efficiency was estimated as a percentage of normalized fluorescent units of bacterial cells relative to the wild type strain or to no aTc addition depending on the experiment. Each condition culture was done in triplicate.

RESULTS

Modulation of RsaE expression uncovers putative RsaE targets

Most characterized sRNAs modulate the stability of targeted mRNAs, directly, or indirectly *via* translation inhibition. To find new RsaE targets, we analyzed the transcriptomes of (i) *S. aureus* HG003 compared to its isogenic

Δ*rsaE* mutant, and (ii) Δ*rsaE* containing *rsaE* controlled by an inducible promoter (P_{tetO}-*rsaE*) grown under non-induced and induced conditions (Supplementary Table S1). For the first couple (wild-type and Δ*rsaE* mutant), both cultures were in steady state and adapted to the presence or absence of RsaE. In contrast, the short induction time (5 min) used with the P_{tetO}-*rsaE* system enabled us to identify primary effects of RsaE accumulation, i.e. putative direct targets, with minimized detection of secondary targets. Transcriptome alterations were determined through differential expression analysis of RNA-seq data.

Twenty-five mRNAs organized in 20 transcription units were both up-regulated in the mutant strain and down-regulated upon RsaE expression and are thus considered as possible targets (Table 1). Among them, expression of *SAOUHSC_00951, SAOUHSC_01138*, *folD, fhs*, *gcvT-gcvPA-gcvPB*, *rocF, citB* and *sucC-sucD* mRNAs was previously reported to be modulated by RsaE in RN6390, a σ^B deficient strain, and direct regulation was demonstrated *in vitro* for *SAOUHSC_00951* and *sucD* mRNAs (16,17). The present results confirm that in HG003, a σ^B repaired strain, the amounts of transcripts encoding enzymes from the TCA cycle and folate pathway are also down-regulated when RsaE is expressed. Interestingly, among the newly identified mRNAs (Table 1), *sucA-sucB, fumC* and *mqo1* mRNAs encode other enzymes of the TCA cycle, namely dihydrolipoamide succinyltransferase and 2-oxoglutarate dehydrogenase, fumarase and malate quinone oxidoreductase, thus extending the regulatory role of RsaE on this pathway. In addition to these, *ald2* mRNA, which encodes an alanine dehydrogenase converting L-alanine to pyruvate, was found to be regulated by RsaE. Also, *rocF*, encoding the arginase that converts arginine to ornithine, was among the mRNAs that were most affected by the absence or accumulation of RsaE (Table 1). These observations suggest that RsaE is also involved in amino acid catabolism.

In vitro trapping of putative RsaE-targets

We used a genome-wide approach to identify substrates that interact directly with RsaE, by extending an *in vitro* method we previously developed to trap sRNA targets using sRNAs as bait (42). Briefly, a synthetic sRNA was produced, biotinylated and fixed to streptavidin-associated magnetic beads. The resulting 'bait' was incubated with total RNA extracts, washed, and RNAs bound to sRNAs were eluted. Recovered RNAs were converted to cDNAs and identified on DNA chips. The method is successful if sRNA targets are well expressed; otherwise, sRNA-targets may be masked by RNA background noise. To overcome this difficulty, (i) RNA-seq rather than DNA-chips was used for target identification, which improved detection (threshold and linearity) and (ii) we hypothesized that nonspecific RNA signals recovered by this protocol would be the same with different sRNAs used as baits; therefore, background noise could be subtracted by a differential analysis of data obtained with several different baits. The modified protocol is called Hybrid-trap-seq (Supplementary Figure S1). Total HG003 RNAs were extracted from 16 growth conditions and pooled together. Hybrid-trap-seq experiments were run in parallel with four baits: RsaE, and three other sRNAs, RNAIII, RsaA and RsaH. The background noise due to nonspecific RNA binding was filtered out from the RsaE Hybrid-trap-seq dataset by a differential analysis using the three other sRNA datasets. This procedure identified eleven mRNAs and one sRNA that accumulated more reads (>10-fold difference) with the RsaE trap than with the three other sRNAs used as baits (Figure 1 and Supplementary Table S2).

RsaE targets SD-like motifs

The twelve RNAs selectively trapped by RsaE are putative primary targets. The regions potentially interacting with RsaE were therefore investigated *in silico*. A predominant motif akin to SD sequences (AAGGGG) was present in seven out of twelve targets, with at least one motif being located at the SD site for the mRNAs. The AAGGGG motif has two exact complementary sequences in RsaE (CCCCTT). Interestingly, the putative RsaE binding motif is present twice in *rocD, rocF*, *icaR* and *rsaOG*, suggesting a possible double seed contact with these putative targets (Figure 2A). The anti-SD-like motifs in RsaE are single-stranded (17) hence accessible to base-pairing, and are located in evolutionary conserved regions (Figure 2B).

Altogether, four independent lines of evidence (motif enrichment, complementarity with sRNA, accessibility and conservation) support the idea that RsaE operates through a seed binding mechanism targeting SD-like regions. A question raised by the use of an SD-like seed region is how specific recognition can be achieved. The RsaE motifs in putative targets (AAGGGG) differ from the canonical *S. aureus* SD motif (AAGGAG, Figure 2C). These differences are matched by specific complementary bases and likely expand from the seed region to allow substrate discrimination as suggested by IntaRNA predicted target sites (Figure 2A and Supplementary Table S4).

Combining experimental approaches to confidently select new RsaE targets

Hybrid-trap-seq experiments are equivalent to genome-wide RNA-RNA retardation assays, with the same *caveat*: do putative targets uncovered *in vitro* correspond to real *in vivo* targets? Among the eleven putative RsaE mRNA targets identified by Hybrid-trap-seq (Table 2), levels of *SAOUHSC_1138* and *rocF* mRNAs were significantly increased in the absence of RsaE and decreased when RsaE expression was induced (Table 1). *rocD*, *ndh2* and *icaR* mRNAs trapped by RsaE showed significantly decreased levels when RsaE expression was induced (0.36, 0.44 and 0.56, FDR < 0.05, respectively). RNA duplexes are predicted *in silico* between RsaE and each of these mRNAs. Altogether, these results suggest a direct interaction of RsaE with *SAOUHSC_1138*, *rocF*, *rocD*, *ndh2* and *icaR* mRNAs (Figure 3).

The level of six other mRNAs identified by Hybrid-trap-seq was not significantly modulated by the RsaE status. In these cases, a direct RsaE interaction with these transcripts may modulate their translation without affecting their stability. However, a complementary sequence with RsaE was only found for RsaOG and *SAOUHSC_02836*,

Table 1. RNAs down-regulated by RsaE

Locus tag*	Gene	Annotation	− RsaE**	+ RsaE***
TCA cycle				
SAOUHSC_01216	*sucC*	Succinyl-CoA synthetase, beta subunit	2.69	0.64
SAOUHSC_01218	*sucD*	Succinyl-CoA synthetase, alpha subunit	2.40	0.63
SAOUHSC_01347	*citB*	Aconitate hydratase 1	1.82	0.38
SAOUHSC_01416	*sucB*	2-oxoglutarate dehydrogenase, E2 component	1.35	0.53
SAOUHSC_01418	*sucA*	2-oxoglutarate dehydrogenase, E1 component	1.36	0.48
SAOUHSC_01983	*fumC*	Fumarate hydratase	1.49	0.42
Malate metabolism				
SAOUHSC_00698		Putative malate transporter	2.31	0.59
SAOUHSC_02647	*mqo1*	Malate:quinone-oxidoreductase	1.38	0.56
Glycine cleavage system				
SAOUHSC_01632	*gcvPB*	Glycine cleavage system P-protein subunit ll	1.37	0.35
SAOUHSC_01633	*gcvPA*	Glycine cleavage system P-protein subunit I	1.40	0.28
SAOUHSC_01634	*gcvT*	Glycine cleavage system T protein	1.42	0.27
Tetrahydrofolate metabolism				
SAOUHSC_01007	*folD*	Tetrahydrofolate dehydrogenase	1.38	0.59
SAOUHSC_01845	*fhs*	Formate-tetrahydrofolate ligase	2.32	0.10
Amino-acid metabolism				
SAOUHSC_01818	*ald2*	Alanine dehydrogenase	3.09	0.48
SAOUHSC_02409	*rocF*	Arginase	2.28	0.31
Others				
SAOUHSC_00094	*sasD*	Cell-wall-anchored protein	1.48	0.34
SAOUHSC_00204	*hmp*	Globin domain containing protein	1.39	0.60
SAOUHSC_00690		Conserved hypothetical protein	1.38	0.63
SAOUHSC_00699	*phrB*	Deoxyribodipyrimidine photolyase	1.82	0.74
SAOUHSC_00838		Truncated conserved hypothetical protein	1.38	0.60
SAOUHSC_00951		Putative RNA ligase or phosphoesterase	2.67	0.56
SAOUHSC_01137	*yjjG*	Putative HAD-hydrolase	1.42	0.50
SAOUHSC_01138		Putative N-acetyltransferase	1.78	0.40
SAOUHSC_01964	*traP*	Signal transduction protein TRAP	1.45	0.43
SAOUHSC_02754		ABC transporter, ATP-binding protein	1.44	0.74

* List of genes differentially expressed (FDR < 0.05, fold change > 1.33 or < 0.75) in both transcriptome comparisons.
** Fold change expression of HG003 Δ*rsaE* relative to wild-type.
*** Fold change expression of HG003 Δ*rsaE* pRMC2RsaE induced relative to not induced.
Fold changes and adjusted *P*-values are available in the GEO database (GEO accession number GSE106457: GSE106456_Supplemental_table_1.txt for the 'Δ*rsaE* relative to wild-type' comparison; GSE106456_Supplemental_table_2.txt for the 'Δ*rsaE* pRMC2RsaE induced relative to not induced' comparison).

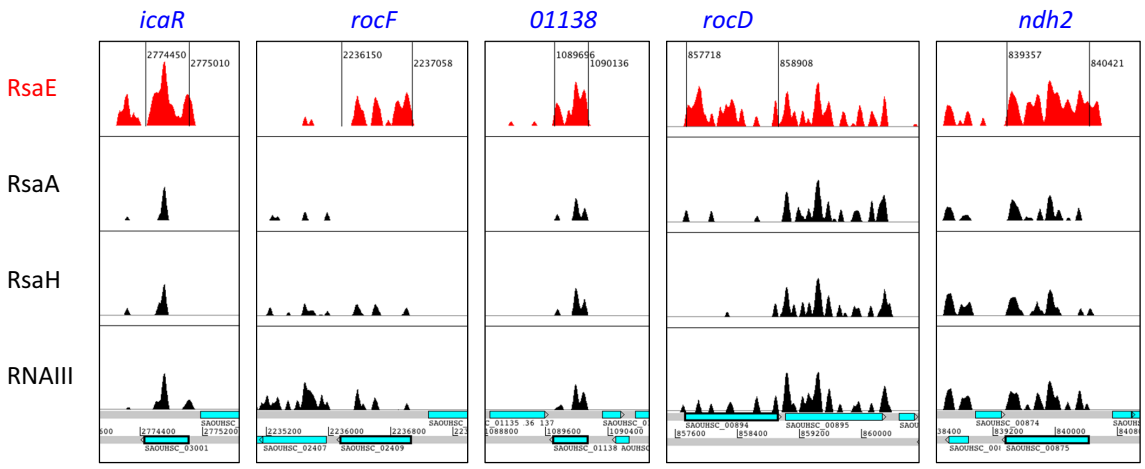

Figure 1. Examples of regions with RsaE-dependent read enrichment. Artemis genome viewer windows showing read density profiles of RsaE-trapped RNAs obtained with Hybrid-trap-seq (Table 1) and found significantly modulated in at least one of the two transcriptomic studies (GSE106457). The red-filled coverage corresponds to RNAs trapped by RsaE. Black-filled coverages correspond to RNAs also retained using unrelated sRNAs (RsaA, RsaH and RNAIII) used to define the level of background noise resulting from nonspecific association. Bottom panel corresponds to genome annotation with blue boxes indicating open reading frames.

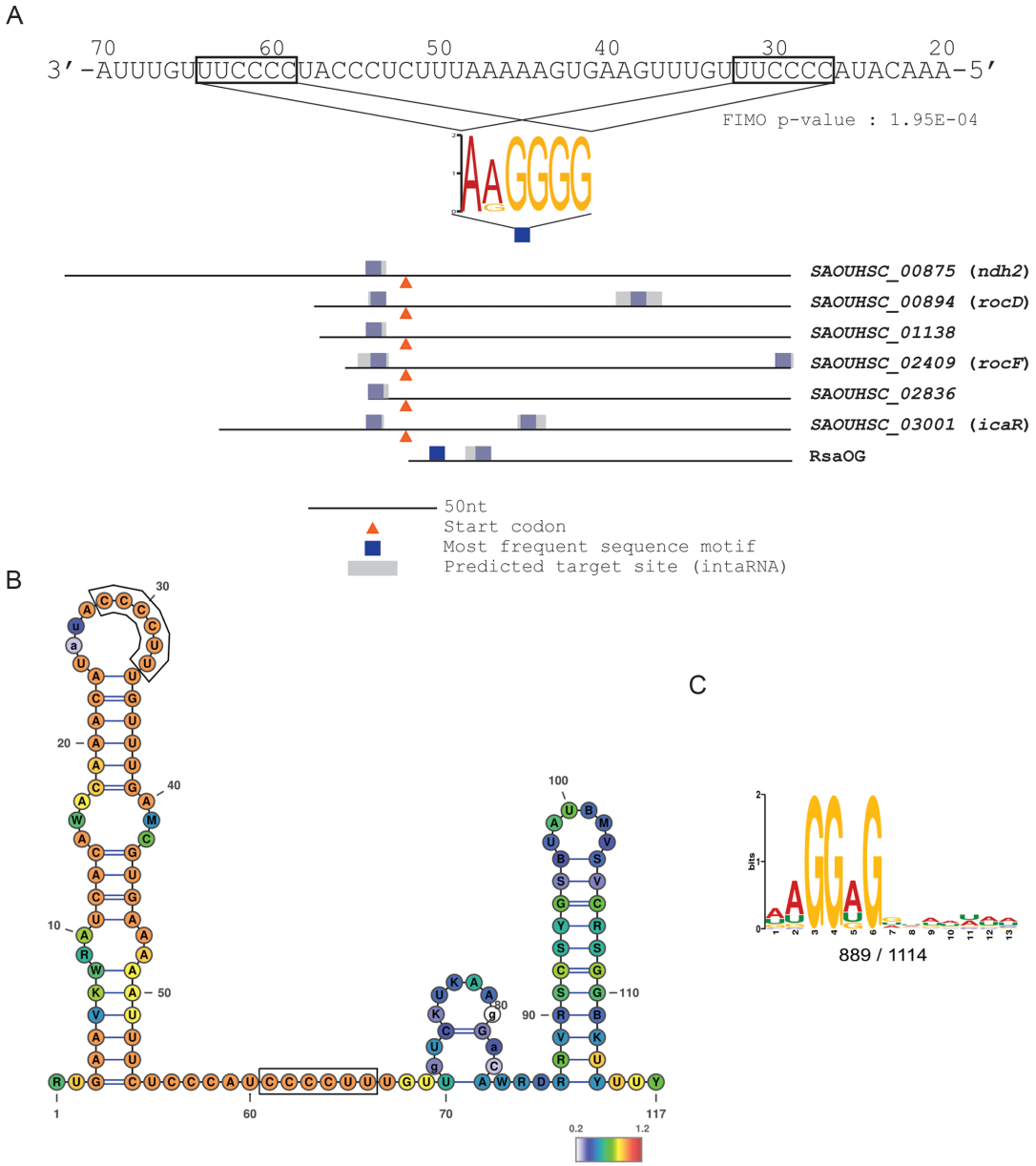

Figure 2. Search of putative RsaE binding motifs. A) MEME (39) sequence motif found in RsaE Hybrid-trap seq targets (Table 2) shown as a colored logo. The motif is connected to its location in target RNAs (colored boxes) and to its complementary site in RsaE. Blue and grey areas in targets correspond to regions of RsaE interaction predicted by MEME (39) and IntaRNA (38), respectively. Orange arrows indicate the position of translation initiation codons. Coordinates of the consensus motif positions on the putative sRNA targets are presented in Supplementary Table S4. B) RsaE secondary structure predicted from a structural alignment of homologous sequences, as provided by the RFAM database (60). Color scale indicates evolutionary conservation at each position (red: most conserved). Boxes around sequences indicate predicted seed matching regions. Structures are drawn using Varna (61). RsaE RFAM entries: RF01820. An experimental structure was reported (17). C) Model for the standard *S. aureus* SD motif, identified by MEME (39) using all HG003 available 5′ UTR regions (see Materials and Method).

which encodes a putative acetyl transferase active on phosphinothricin, a glutamate analogue (45).

rocF and *SAOUHSC_1138* mRNAs, found by three approaches, are most likely RsaE direct targets (Figure 3). *rocD* mRNA encodes the ornithine-oxo-acid transaminase and RocD acts together with RocF and RocA to interconvert arginine to glutamate (30). *rocF* and *rocD* are genetically unlinked but are both down-regulated by RsaE and their mRNAs were also trapped *in vitro* by RsaE; this functional convergence reinforces our hypothesis of a direct involvement of RsaE in the control of arginine metabolism.

Two motifs of RsaE contribute independently to the down-regulation of its substrates

The repetition of identical binding motifs is an unusual feature for sRNAs. We therefore tested the contribution of each CCCCUU sequence of RsaE on target degra-

Table 2. RsaE-trapped RNAs

Locus tag	Gene	Annotation	Fold change
SAOUHSC_03001	*icaR*	*ica* operon transcriptional regulator	46.6
	rsaOG	CcpA regulated sRNA	31.1
SAOUHSC_01546		Conserved hypothetical phage protein	25.5
SAOUHSC_01016	*purN*	Phosphoribosylglycinamide formyltransferase	20.1
SAOUHSC_02409	*rocF*	Arginase	19.4
SAOUHSC_02836		Acetyltransferase (GNAT) family protein	18.9
SAOUHSC_01543		Phage phi related protein	16.1
SAOUHSC_01138		Putative N-acetyltransferase	11.9
SAOUHSC_00875	*ndh2*	Pyridine nucleotide-disulfide oxidoreductase	11.9
SAOUHSC_01017	*purH*	Phosphoribosylaminoimidazolecarboxamide formyltransferase / IMP cyclohydrolase	10.9
SAOUHSC_00894	*rocD*	Ornithine aminotransferase	10.7
SAOUHSC_00819	*cspC*	Cold shock domain protein	10.4

Full results are available under GEO accession number GSE106327.

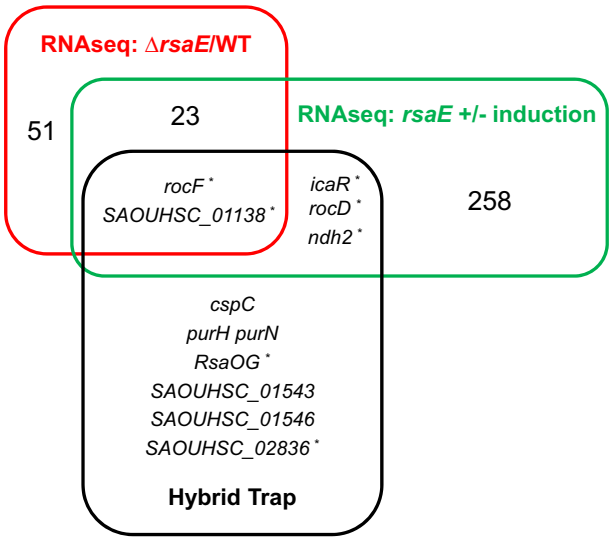

Figure 3. Combining experiments to uncover RsaE-targets. Venn diagram showing the overlap between different methods for prediction of putative RsaE targets: transcriptomic (Δ*rsaE versus* HG003, red; Δ*rsaE* pRsaE with *versus* without induction, green; threshold 1.33, $P < 0.05$) and Hybrid-trap-seq experiments (black, min. 10-fold variation). *, RNAs with G-rich motifs.

dation. For this study, we chose to monitor *rocF* and *SAOUHSC_01138* mRNAs as the most likely primary RsaE targets (Figure 3) as well as *rocD* mRNA which is involved in the same metabolic pathway as *rocF* mRNA. We confirmed their down-regulation upon RsaE induction by Northern blots (Figure 4B) and qRT-PCR (Supplementary Table S5). Two bands were detected when *rocF* mRNA was probed. They may come from either alternative promoters or processing events. The lower band is predominant and the higher is moderately affected by RsaE; however, both were summed for quantification. The first CCCCTT motif of *rsaE* was changed to CTCCAA leading to the *rsaE1* allele (Figure 4A). Induction of *rsaE1* still resulted in the decrease of *rocF*, *SAOUHSC_01138* and *rocD-gudB* mRNAs, showing that the first motif was not essential for RsaE regulatory activity, although the *rsaE1* allele was expressed to a lesser amount (Figure 4B). Mutations in the first motif likely affect RsaE stability, judging by expression levels. The second CCCCTT *rsaE* motif was also changed to CTCCAA to create the *rsaE2* allele (Figure 4A). Induction of *rsaE2* also resulted in the disappearance of *rocF*, *SAOUHSC_01138* and *rocD-gudB* mRNAs showing that the second motif was not essential for RsaE activity against these mRNAs (Figure 4B). However, induction of a *rsaE* allele mutated for both motifs (*rsaE1&2*) did not affect mRNA quantities of the three targets (Figure 4B). We concluded that the two RsaE motifs can act independently against *rocF* and *rocD-gudB* mRNAs. However, on *SAOUHSC_1138* mRNA, RsaE motif 1 was more active than RsaE motif 2 (Figure 4B) indicating that both motifs may act differently according to substrates.

RsaE targets mRNA SD sequence and translation

Some mRNAs targeted by RsaE have two cognate putative RsaE binding sites (Figure 2A and Supplementary Figure S2). We tested whether changes in these sites on the *rocF* mRNA alter RsaE activity. The first putative binding motif is within a non-canonical SD sequence AAGGGGG (Figure 5A). The motif was changed to TTGGAGG, leading to *rocF1* allele (Figure 5B). This modification created a canonical SD sequence to maintain *rocF* translation. The second putative motif was 141 nucleotides downstream from the translational start codon. It was changed from AAGGGGG to TTGGAGG leading to *rocF2* allele and consequently altering the RocF amino acid composition (K49L and G50E). The combination of both alleles, *rocF1&2*, was also constructed (Figure 5B). All these mutations were introduced by allelic replacement at the *rocF* locus in HG003 Δ*rsaE*. These strains were then transformed with pRMC2RsaE and the amount of *rocF* mRNA was assayed by northern blot (Figure 5C). As for wild-type *rocF* mRNA (Figure 4B), two bands were detected when *rocF* mRNA was probed, but mutations affecting *rocF* mRNA resulted in an increase of the higher band. Mutations may affect *rocF* mRNA structure and translation, which in turn affect the ratio between each band. As indicated above, both *rocF* mRNA bands were summed for quantification. *rocF* downregulation by RsaE was effective for *rocF2* but less for *rocF1* and *rocF1&2* carrying strains, suggesting that RsaE preferentially pairs to the *rocF* mRNA SD sequence. One prediction from this pairing is that mu-

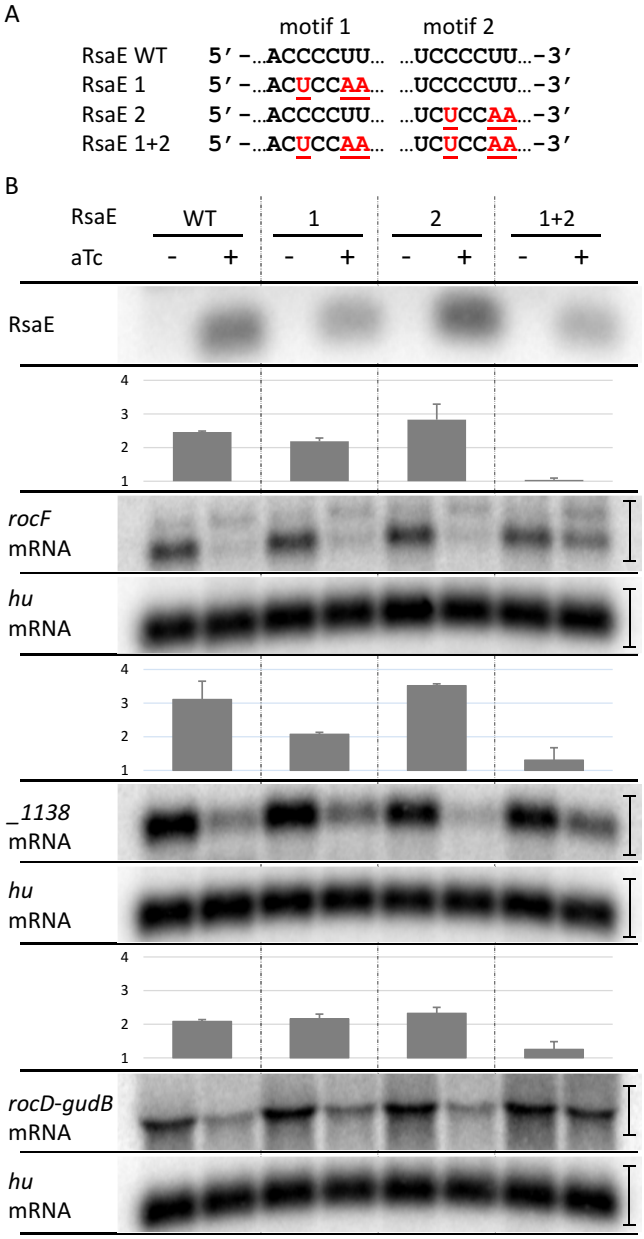

Figure 4. Two RsaE repeated motifs contribute independently to its activity. (**A**) RsaE mutations introduced in motifs 1 and 2. Wild-type sequence is in black, mutations are in red. (**B**) Effect of RsaE and mutated RsaE induction on *rocF*, *rocD* and *SAOUHSC_1138* mRNA levels. Total RNAs were extracted from strains expressing conditionally RsaE upon the addition of aTc (1 μM) to the medium. (–), without aTc addition; (+), with 5 min aTc induction. RsaE, *rocF* mRNA, *rocD* mRNA and *SAOUHSC_1138* RNAs were visualized by Northern blot experiments as indicated. *Hu* mRNA was used as a loading control. Histograms indicate target repression folds expressed as a ratio of target intensity upon non-induction relative to induction of *rsaE* and mutated *rsaE*. Vertical bars on the right indicate the width of regions around Northern bands selected to calculate ^{32}P signal intensity with ImageJ software. *rocF* mRNA signals are located between markers 1000 and 1500 nt. Error bars represent standard deviations of the repression folds calculated using biological duplicates.

tations in *rsaE* restoring base-pair complementarity with *rocF1&2* would restore RsaE activity. To test this, HG003 Δ*rsaE rocF1&2* was transformed with pRMC2RsaE1&2. Induction of RsaE1&2 led indeed to a decreased quantity of *rocF1&2* mRNA (Figure 5C). The effect with the mutated alleles is less pronounced than with wild-type alleles, possibly due to structural constraints that affect pairing, and/or susceptibility of the complex to ribonucleases. Altogether, these experiments demonstrate an *in vivo* direct pairing between RsaE and the *rocF* mRNA SD sequence suggesting that RsaE acts at the level of translation and indirectly affects stability.

The SD region was also the predicted RsaE pairing site for other mRNA targets (Figure 2A and Supplementary Figure S2) suggesting that they are also regulated by RsaE at the translation level. To determine if this is indeed the case, translational fusions between *SAOUHSC_1138* and *rocD* mRNA 5′-end region and *lacZ* were constructed and introduced in (i) Δ*rsaE* and its parental strain and (ii) in Δ*rsaE* pRMC2RsaE. Absence of RsaE lead to an increase of β-galactosidase activity, while a 15-min induction of *rsaE* resulted in a significant decrease of β-galactosidase activity, confirming that RsaE acts negatively on *rocD* and *SAOUHSC_01138 mRNA* translation (Supplementary Figure S3).

RsaE contributes to amino acid catabolism regulation

Despite being highly conserved within the Firmicutes phylum and having putative and demonstrated targets, no physiological phenotype was thus far associated with an *rsaE* deletion. Indeed, no competitive growth difference between HG003 and its Δ*rsaE* derivative was observed in rich media. However, if RsaE functions to repress amino acid catabolism, we would predict that Δ*rsaE* would have an increased growth rate in media containing only amino acids as a carbon source. Indeed, the Δ*rsaE* strain had a faster growth rate than HG003 in CDM, which contains amino acids as the sole carbon source (Figure 6). Of those amino acids that are known to be rapidly catabolized in CDM (30), glutamate (Figure 6) as well as threonine, serine, alanine, glycine, proline and aspartate were catabolized more rapidly during exponential phase in the absence of RsaE (Supplementary Figure S4). When percent amino acid consumed were corrected for growth, the rates of consumption were not significantly different between Δ*rsaE* and WT HG003 documenting that the amount of amino acid consumed between the two strains was proportional to the biomass (Supplementary Figure S5). Collectively, these data suggest that the absence of RsaE leads to the upregulation of enzymes contributing to amino acid catabolism, which in turn stimulates growth rate.

DISCUSSION

Finding sRNA targets and function remain challenging. Here, by combining transcriptomic analyses, *in vitro* trapping and bioinformatics, we bring to light new RsaE features.

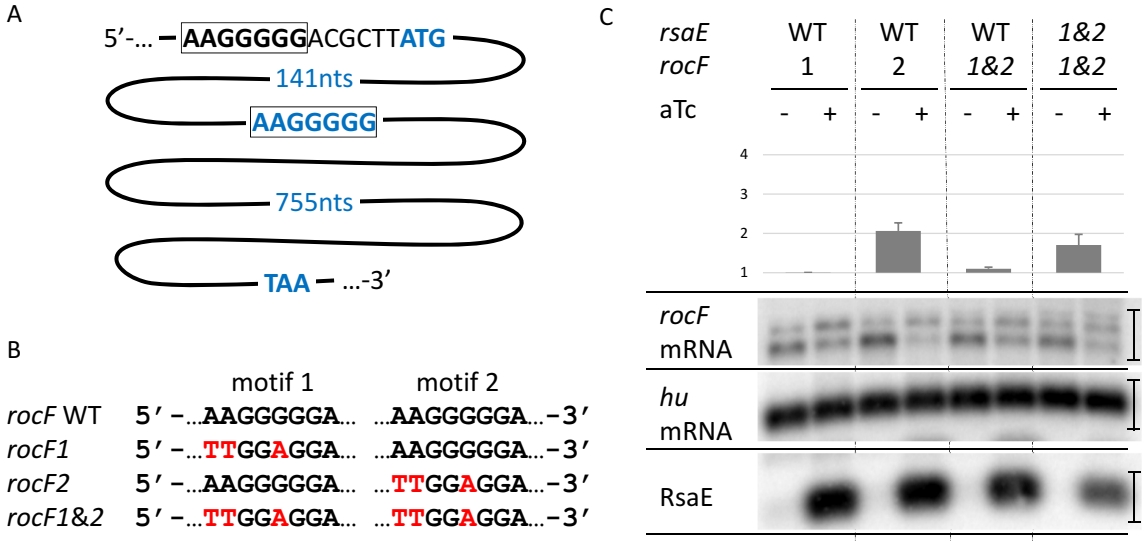

Figure 5. RsaE targets the SD sequence of *rocF* mRNA. (**A**) Schematic representation of the two duplicated motifs complementary of RsaE in *rocF* mRNA. The first one is within the SD sequence (black and squared), the second one within the coding sequence (blue and squared). (nts), nucleotides. (**B**) *rocF* mutations introduced in motifs 1 and 2. The wild-type sequence is in black, mutations are in red. Mutated *rocF* alleles were introduced in HG003 chromosome by allelic exchange at the *rocF* locus. (**C**) Effect of RsaE and RsaE1&2 induction on *rocF* and mutated *rocF* mRNAs. For figure explanation and experimental conditions see Figure 4 legend.

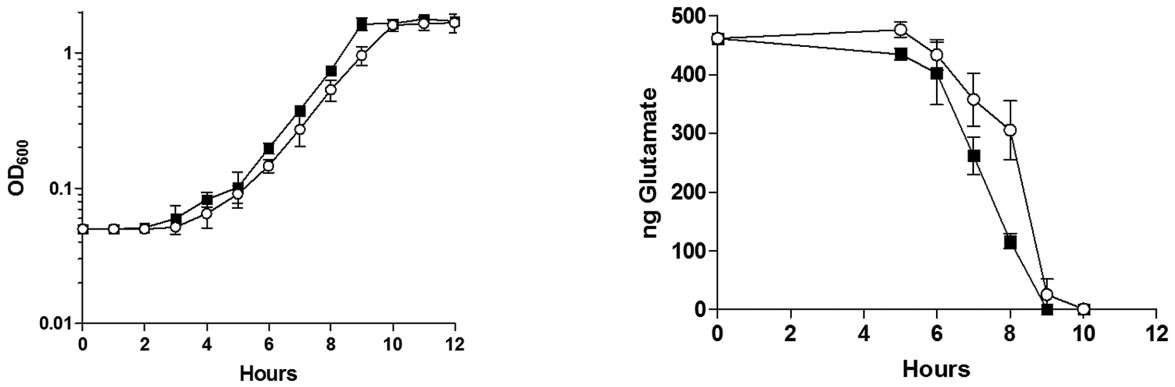

Figure 6. Growth and glutamate consumption of HG003 and HG003 Δ*rsaE*. HG003 (white dot) and HG003 Δ*rsaE* (black square). Left panel: growth in CDM. HG003 and HG003 Δ*rsaE* doubling time are 69 min (±1.1) and 58 min (±1.8), respectively. Right panel: Glutamate consumption following aerobic growth in CDM. Glutamate concentrations (ng/μl) were measured in the supernatant at the indicated time of growth. Experiments were performed three times and the error bars represent the standard deviation of the means.

RsaE is a paradigm for regulatory RNAs in Firmicutes

RsaE is remarkably conserved in the *Staphylococcaceae* and *Bacillaceae* families (Supplementary Table S6) and has been studied in two representative species *S. aureus* and *B. subtilis*, respectively. In *S. aureus*, RsaE modulates transcripts of enzymes involved in the TCA cycle, the glycine cleavage system, and tetrahydrofolate metabolism (16,17). In *B. subtilis*, the RsaE homolog RoxS downregulates transcripts associated with oxido-reduction reactions and is proposed to partly control NAD^+/NADH balance (14,15).

Our transcriptomic analyses provide a confirmation of previously proposed RsaE targets. They also reveal additional RsaE-regulated steps of the TCA cycle (i.e. *sucAB*, *fumC* and *mqo1*). All TCA cycle steps except succinate-fumarate conversion are subject to RsaE downregulation. In addition, importantly, we provide new evidence that RsaE regulates arginine catabolism.

RsaE targets the arginine catabolism by a direct interaction with the *rocF* mRNA

RsaE affects numerous transcripts, but to date, formal demonstrations of physiological sRNA/mRNA interactions were limited by difficulties in performing staphylococcal genetic studies. *In vitro* evidence based on gel retardation assays and toe-printing experiments, associated with transcriptomic and proteomic studies, indicated that RsaE acts by a direct pairing with *sucCD*, *SA0873* (*SAOUHSC_00951*), *opp3B* (17) and *opp3A* mRNAs (16). Here, the *in vivo* effect of RsaE on *rocF* mRNA was

demonstrated by transcriptomic, northern blot and qRT-PCR experiments. Further evidence for a direct interaction was given *in vitro* by a RsaE-dependent trapping of *rocF* mRNA, and *in vivo* by a targeted mutagenesis on predicted intermolecular RsaE/*rocF* mRNA pairings.

The RsaE duplicated motifs can have common and specific targets

Some sRNAs exert their regulatory activity by pairing to targets with two complementary regions [*e.g.* (46)]. However, RsaE harbors two identical motifs that may recognize identical target sequences. In *B. subtilis*, pairing of RoxS with its targets was addressed *via* a mutational study of C-rich regions (CRR1 to 4) (14,15). RoxS and RsaE sequences are almost identical (except for their terminators), and two repeat sequences of 10 nucleotides, referred to here as RsaE motifs 1 and 2, correspond to CRR1 and CRR3 in *B. subtilis*, respectively. Motif 1 is within a loop of a stem–loop structure while motif 2 is an unpaired sequence between two stems (Figure 3B). Both sequences are predicted to pair to complementary G-rich sequences and indeed we observed that both motifs 1 and 2 can exert independent regulatory functions. However, motif 1 had a stronger effect on one target (*SAOUHSC_01138* mRNA), suggesting that presentation of the motif by a stem may promote the sRNA/mRNA pairing. On the contrary, RoxS requires the integrity of CRR3 (equivalent to motif 2) but not CRR1 to inhibit the formation of a translation initiation complex on the *ppnKB* target mRNA (14). Also, RoxS CRR3 but not CRR1 was shown to be involved in *yflS* RNA recognition (15). The presence of two conserved motifs in RsaE and its orthologs is probably not fortuitous, as they can target the same substrate (e.g. motifs 1 and 2 on *rocF* mRNA) or dedicated substrates (e.g. CCR3 on *ppnKB* mRNA). Sequences surrounding each motif might extend RsaE/mRNA pairing and be essential for recognition of certain substrates (Supplementary Figure S2 and Supplementary Table S4). Note that IntaRNA rank first RsaE motif 2 for interactions with *rocF* and *rocD* mRNAs (Supplementary Figure S2) while both motifs seem equivalent for down-regulation. Numerous factors not considered by target prediction software such as RNA chaperones, RNA helicases, RNA sponges and nucleases strongly affect the sRNA/mRNA interactions.

How RsaE binding leads to substrate regulation remains to be elucidated. In *B. subtilis*, RNase Y contributes to RoxS processing and RoxS-target degradation (14). However, in a *S. aureus* strain lacking RNase Y, RsaE quantity was not increased and no significant RsaE-target enrichment was observed (47). In contrast, RsaE and putative substrates where found associated with RNase III, suggesting a role for this double strand specific RNase in RsaE-dependent regulations (48).

RsaE and amino acid metabolism

The *gcvT-gcvPA-gcvPB* operon encodes glycine decarboxylase enzymes providing methylene groups for the one-carbon metabolism and *ald2* encodes an alanine dehydrogenase, a deaminating enzyme converting alanine to pyruvate. The corresponding mRNAs of both pathways are down-regulated by RsaE. This observation is also true for the arginase *rocF* mRNA. In agreement with these results, in the absence of RsaE, HG003 grows at a faster rate in media containing amino acids as the sole carbon sources. It is known that pathways essential to growth on secondary carbon sources, such as catabolic pathways generating pyruvate from alanine and glycine, and the TCA cycle are regulated by RsaE. These results, in addition to the demonstrated *rocF* regulation, suggest that RsaE is a general regulator of amino acid catabolism. Besides repressing several enzymes using NAD as cofactor, RsaE reduces amino acid catabolism and may consequently limit the feeding of the TCA cycle (Figure 7). If so, RsaE would contribute to control the NAD^+/NADH ratio, a role proposed for RoxS in *B. subtilis* (15) and therefore conserved among distantly related Firmicutes.

Evidence for overlapping RsaE and SrrAB regulons

RsaE expression requires the two-component system SrrAB (14). Low oxygen concentrations or the presence of nitric oxide (NO) is sensed by the membrane protein SrrB, which activates SrrA *via* a phosphorelay, consequently stimulating *rsaE* transcription. In *B. subtilis*, RoxS expression is enhanced by ResDE (SrrAB orthologs), but also repressed by Rex, a redox sensing regulator activated by high NAD^+/NADH ratio (14,15). The *roxS* Rex binding site is strictly conserved in *rsaE,* suggesting that in *S. aureus*, Rex similarly represses *rsaE* expression (15). If so, full expression of RsaE would require SrrAB activation (low O_2 or NO) and a low NAD^+/NADH ratio. High levels of NAD^+, which is a cofactor for many enzymes downregulated by RsaE (Figure 7) would induce Rex-mediated repression of RsaE in low oxygen conditions. Consequently, these NAD^+ consuming metabolic pathways would not be shut down by RsaE.

Disruption of the *srrAB* operon (also named *srhSR*) leads to altered growth in anaerobic conditions (49). A proteomic study of *S. aureus* strain WCUH29 revealed a number of proteins that significantly increase in the absence of SrrAB: in aerobic conditions, SucD, RocD, RocF and SAOUHSC_01138 (alias YlbP) and in anaerobic conditions, SucC, SucD, RocD, RocF, SAOUHSC_01138, LctE, Ndh, Ald2, CitB, FumC (49). With the exception of LctE, all upregulated proteins in Δ*srrAB* are also down-regulated by RsaE. Cross-comparison of Throup *et al.* with the current work suggests that RsaE is the main negative effector of the SrrAB pathway. Recent studies comparing the *srrAB* and wild-type transcriptomes show a limited overlap with Throup *et al.* (50,51), but conditions and strains are different. As RsaE binds to SDs and its inhibitory activity is first on translation, proteomics provides an efficient readout of RsaE activation.

RsaE controls CcpA-regulated genes

CcpA is a key regulator of carbon metabolism adaptation in Firmicutes. It represses genes associated with secondary carbon source acquisition or utilization, including TCA cycle and amino acid related genes (30,52–54). Many of these genes are also RsaE-regulated (Figure 7). RsaE, by acting post-transcriptionally, may synergistically shut off gene expression or ensure a negative control during oxygen deprivation on a subset of CcpA-regulated

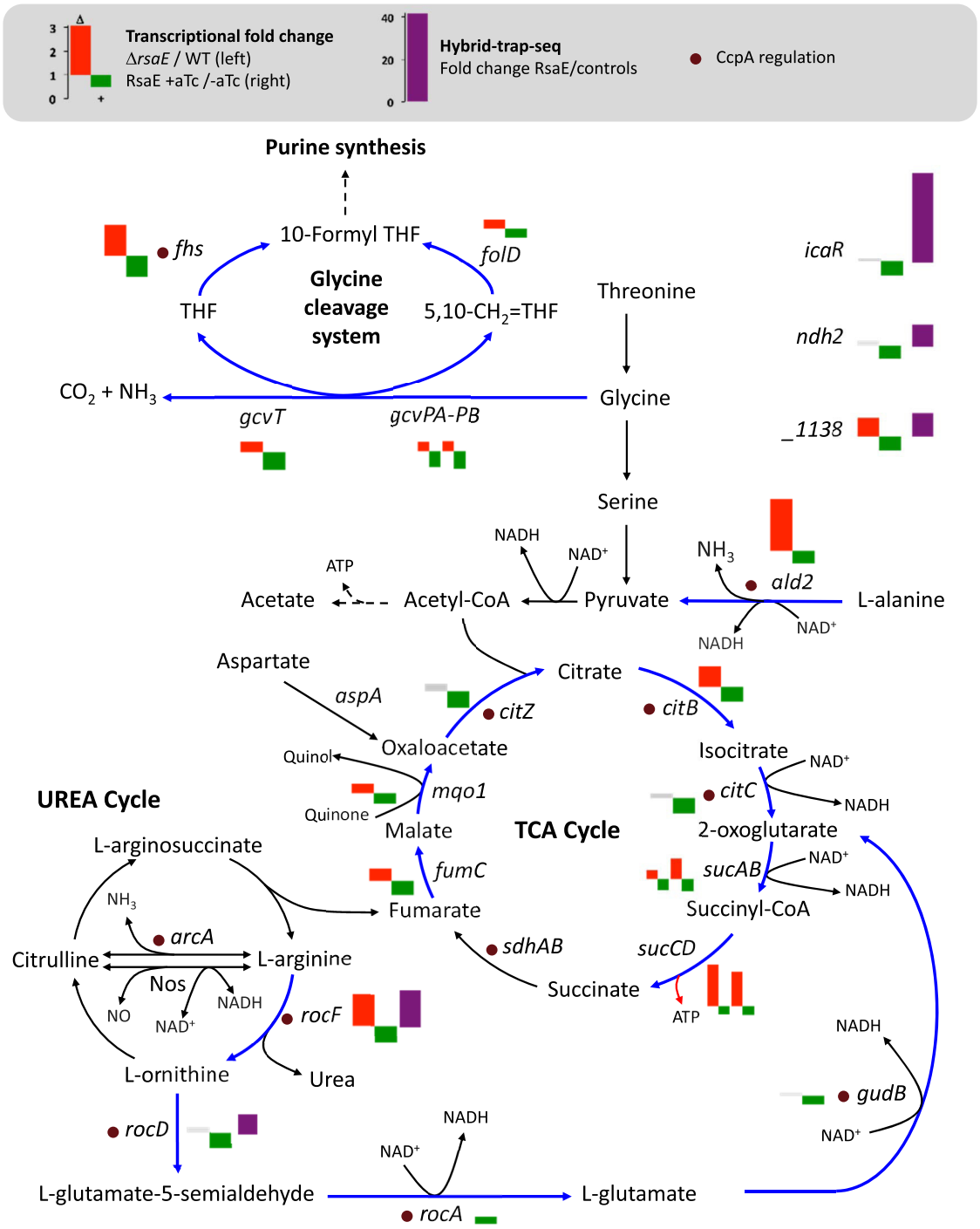

Figure 7. Metabolic pathways associated with RsaE regulations. RsaE downregulates mRNAs (blue arrows) associated with the glycine cleavage system, the TCA cycle, the urea cycle and amino acid metabolisms. Histograms next to relevant gene names represent transcriptional change values from Table 1 (red boxes correspond to genes up-regulated in Δ*rsaE*/WT experiments, green boxes to genes down-regulated upon *rsaE* induction, and grey boxes to genes not significantly regulated). Some RsaE direct interactions on mRNAs are supported by *in vitro* evidences; histograms with purple boxes correspond to values from Table 2 (Hybrid-trap-seq data). Purple dots indicate CcpA-regulated genes.

genes. The sRNA RsaOG (43,55) [also known as RsaI (17)] is CcpA-regulated (56, BioRxiv: https://doi.org/10.1101/278127) and trapped by RsaE (Table 2). Using an MS2-affinity purification approach, P. Romby, I. Caldelari and coworkers recently showed that RsaOG binds to several sRNAs including RsaE to possibly regulate them (BioRxiv: https://doi.org/10.1101/278127). Consequently, RsaOG could connect RsaE activity to CcpA regulation.

RsaE function conservation across species

A computer search for putative RsaE targets in *Staphylococcus epidermidis* (RP62A) and *B. subtilis* using RNApredator (58) revealed a remarkable target conservation, an unusual feature for sRNAs.

In *S. epidermidis*, *sucD*, *ylbP* (*SERP0741*), *traP* (*SERP1369*), *rocD*, *citB* (*SERP0921*), *yjcG* (*SERP0604*) and *icaR* mRNAs are among the best matches of SD regions targeted by RsaE (Supplementary Table S7).

Although *B. subtilis* is distantly related to *S. aureus*, some common targets of RoxS and RsaE, such as *sucCD* mRNA, were confirmed in both species. Moreover, *sucCD* mRNA is likely an RsaE target also in *S. epidermidis*. (Supplementary Table S7). This example in itself supports the idea of a conserved RsaE function across distant species.

In *B. subtilis*, the arginine catabolic genes have a different genetic organization compared to *S. aureus*: the transcription of *rocABC* and *rocDEF* operons is σ^L-dependent and under the control of RocR and AhrC (59). Interestingly, the *B. subtilis* arginine catabolic pathway is possibly controlled by RoxS. *rocA* and *rocG* (alias *gudB* in *S. aureus*) mRNAs are downregulated by RoxS (14). In addition, *rocD* SD is a predicted RoxS target (Supplementary Table S7). RoxS activity on *rocD* mRNA likely affect *rocF* (named *argI* in *B. subtilis*) expression as both genes are in the same operon. These observations suggest that the RsaE regulation of the arginine catabolic pathway may also be conserved between *Staphylococcaceae* and *Bacillaceae*.

CONCLUSION

RsaE is a global and highly conserved regulator of central metabolic functions, including the TCA cycle, the glycine cleavage pathway, tetrahydrofolate metabolism and the catabolism of several amino acids including arginine. It affects numerous CcpA regulated genes. RsaE would be a negative effector of the SrrAB regulon, and expectedly be more expressed when oxygen and NAD^+ levels are low (14,15). RsaE operates *via* two seed motifs that may act differentially according to targets. It is likely that RsaE regulation is conserved and acts on the same pathways in other Firmicutes.

DATA AVAILABILITY

Sequencing data from transcriptomes and Hybrid-trap-seq have been deposited in GEO under the accession number GSE106457.

SUPPLEMENTARY DATA

Supplementary Data are available at NAR Online.

ACKNOWLEDGEMENTS

We thank Tim Foster and Friedrich Götz for providing plasmids and strains. We thank Sandy Gruss, Steven Carson and Vinai Thomas for critical reading of the manuscript. We thank Sandy Gruss, David Halpern, Elise Borezée-Durant and Hoega Arden for helpful discussions and warm support. Lastly, we thank Valerie Shostrom for statistical analyses. This work has benefited from the facilities and expertise of the high throughput-sequencing platform of IMAGIF (http://www.i2bc.paris-saclay.fr) and of the INRA MIGALE bioinformatics platform (http://migale.jouy.inra.fr) for computational resources.

FUNDING

Agence Nationale pour la Recherche [ANR-2012-BLAN-1602 (Duplex-Omics); ANR-15-CE12-0003 (sRNA-Fit)]; Fondation pour la Recherche Médicale [DBF20160635724]; National Institutes of Health [NIH/NIAID P01AI083211]. Funding for open access charge: Agence Nationale pour la Recherche [ANR-15-CE12-0003].

Conflict of interest statement. None declared.

REFERENCES

1. Bischoff,M., Dunman,P., Kormanec,J., Macapagal,D., Murphy,E., Mounts,W., Berger-Bachi,B. and Projan,S. (2004) Microarray-based analysis of the *Staphylococcus aureus* sigmaB regulon. *J. Bacteriol.*, **186**, 4085–4099.
2. Shaw,L.N., Lindholm,C., Prajsnar,T.K., Miller,H.K., Brown,M.C., Golonka,E., Stewart,G.C., Tarkowski,A. and Potempa,J. (2008) Identification and characterization of sigma, a novel component of the *Staphylococcus aureus* stress and virulence responses. *PLoS One*, **3**, e3844.
3. Tuchscherr,L. and Loffler,B. (2016) *Staphylococcus aureus* dynamically adapts global regulators and virulence factor expression in the course from acute to chronic infection. *Curr. Genet.*, **62**, 15–17.
4. Seidl,K., Stucki,M., Ruegg,M., Goerke,C., Wolz,C., Harris,L., Berger-Bachi,B. and Bischoff,M. (2006) *Staphylococcus aureus* CcpA affects virulence determinant production and antibiotic resistance. *Antimicrob. Agents Chemother.*, **50**, 1183–1194.
5. Majerczyk,C.D., Dunman,P.M., Luong,T.T., Lee,C.Y., Sadykov,M.R., Somerville,G.A., Bodi,K. and Sonenshein,A.L. (2010) Direct targets of CodY in Staphylococcus aureus. *J. Bacteriol.*, **192**, 2861–2877.
6. Pohl,K., Francois,P., Stenz,L., Schlink,F., Geiger,T., Herbert,S., Goerke,C., Schrenzel,J. and Wolz,C. (2009) CodY in *Staphylococcus aureus*: a regulatory link between metabolism and virulence gene expression. *J. Bacteriol.*, **191**, 2953–2963.
7. Felden,B., Vandenesch,F., Bouloc,P. and Romby,P. (2011) The *Staphylococcus aureus* RNome and its commitment to virulence. *PLoS Pathog.*, **7**, e1002006.
8. Durica-Mitic,S., Gopel,Y. and Gorke,B. (2018) Carbohydrate Utilization in Bacteria: Making the Most Out of Sugars with the Help of Small Regulatory RNAs. *Microbiol. Spectrum*, **6**, RWR-0013–2017.
9. Barquist,L. and Vogel,J. (2015) Accelerating discovery and functional analysis of small RNAs with new technologies. *Annu. Rev. Genet.*, **49**, 367–394.
10. Liu,W., Rochat,T., Toffano-Nioche,C., Le Lam,T.N., Bouloc,P. and Morvan,C. (2018) Assessment of Bona Fide sRNAs in *Staphylococcus aureus*. *Front Microbiol*, **9**, 228.
11. Storz,G., Vogel,J. and Wassarman,K.M. (2011) Regulation by small RNAs in bacteria: expanding frontiers. *Mol. Cell*, **43**, 880–891.
12. Novick,R.P. and Geisinger,E. (2008) Quorum sensing in staphylococci. *Annu. Rev. Genet.*, **42**, 541–564.
13. Gautheret,D. (2014) *Handbook of RNA Biochemistry*. Wiley-VCH Verlag GmbH & Co. KGaA, pp. 595–618.

14. Durand,S., Braun,F., Lioliou,E., Romilly,C., Helfer,A.C., Kuhn,L., Quittot,N., Nicolas,P., Romby,P. and Condon,C. (2015) A nitric oxide regulated small RNA controls expression of genes involved in redox homeostasis in *Bacillus subtilis*. *PLos Genet.*, **11**, e1004957.
15. Durand,S., Braun,F., Helfer,A.C., Romby,P. and Condon,C. (2017) sRNA-mediated activation of gene expression by inhibition of 5′-3′ exonucleolytic mRNA degradation. *eLife*, **6**, e23602.
16. Bohn,C., Rigoulay,C., Chabelskaya,S., Sharma,C.M., Marchais,A., Skorski,P., Borezee-Durant,E., Barbet,R., Jacquet,E., Jacq,A. *et al.* (2010) Experimental discovery of small RNAs in *Staphylococcus aureus* reveals a riboregulator of central metabolism. *Nucleic. Acids. Res.*, **38**, 6620–6636.
17. Geissmann,T., Chevalier,C., Cros,M.J., Boisset,S., Fechter,P., Noirot,C., Schrenzel,J., Francois,P., Vandenesch,F., Gaspin,C. *et al.* (2009) A search for small noncoding RNAs in *Staphylococcus aureus* reveals a conserved sequence motif for regulation. *Nucleic. Acids. Res.*, **37**, 7239–7257.
18. Bouloc,P. and Repoila,F. (2016) Fresh layers of RNA-mediated regulation in Gram-positive bacteria. *Curr. Opin. Microbiol.*, **30**, 30–35.
19. Bohn,C., Rigoulay,C. and Bouloc,P. (2007) No detectable effect of RNA-binding protein Hfq absence in *Staphylococcus aureus*. *BMC Microbiol.*, **7**, 10.
20. Rochat,T., Delumeau,O., Figueroa-Bossi,N., Noirot,P., Bossi,L., Dervyn,E. and Bouloc,P. (2015) Tracking the Elusive Function of *Bacillus subtilis* Hfq. *PLoS One*, **10**, e0124977.
21. Song,J., Lays,C., Vandenesch,F., Benito,Y., Bes,M., Chu,Y., Lina,G., Romby,P., Geissmann,T. and Boisset,S. (2012) The expression of small regulatory RNAs in clinical samples reflects the different life styles of *Staphylococcus aureus* in colonization vs. infection. *PLoS One*, **7**, e37294.
22. Mashruwala,A.A., Guchte,A.V. and Boyd,J.M. (2017) Impaired respiration elicits SrrAB-dependent programmed cell lysis and biofilm formation in *Staphylococcus aureus*. *eLife*, **6**, e23845.
23. Herbert,S., Ziebandt,A.K., Ohlsen,K., Schafer,T., Hecker,M., Albrecht,D., Novick,R. and Gotz,F. (2010) Repair of global regulators in *Staphylococcus aureus* 8325 and comparative analysis with other clinical isolates. *Infect. Immun.*, **78**, 2877–2889.
24. Le Lam,T.N., Morvan,C., Liu,W., Bohn,C., Jaszczyszyn,Y. and Bouloc,P. (2017) Finding sRNA-associated phenotypes by competition assays: an example with Staphylococcus aureus. *Methods*, **117**, 21–27.
25. Corrigan,R.M. and Foster,T.J. (2009) An improved tetracycline-inducible expression vector for *Staphylococcus aureus*. *Plasmid*, **61**, 126–129.
26. Huntzinger,E., Boisset,S., Saveanu,C., Benito,Y., Geissmann,T., Namane,A., Lina,G., Etienne,J., Ehresmann,B., Ehresmann,C. *et al.* (2005) *Staphylococcus aureus* RNAIII and the endoribonuclease III coordinately regulate spa gene expression. *EMBO J.*, **24**, 824–835.
27. Poyart,C. and Trieu-Cuot,P. (1997) A broad-host-range mobilizable shuttle vector for the construction of transcriptional fusions to beta-galactosidase in gram-positive bacteria. *FEMS Microbiol. Lett.*, **156**, 193–198.
28. Gibson,D.G., Young,L., Chuang,R.Y., Venter,J.C., Hutchison,C.A. 3rd and Smith,H.O. (2009) Enzymatic assembly of DNA molecules up to several hundred kilobases. *Nat. Methods*, **6**, 343–345.
29. Hussain,M., Hastings,J.G. and White,P.J. (1991) A chemically defined medium for slime production by coagulase-negative staphylococci. *J. Med. Microbiol.*, **34**, 143–147.
30. Halsey,C.R., Lei,S., Wax,J.K., Lehman,M.K., Nuxoll,A.S., Steinke,L., Sadykov,M., Powers,R. and Fey,P.D. (2017) Amino acid catabolism in *Staphylococcus aureus* and the function of carbon catabolite repression. *mBio*, **8**, e01434-16.
31. Jestin,J.L., Deme,E. and Jacquier,A. (1997) Identification of structural elements critical for inter-domain interactions in a group II self-splicing intron. *EMBO J.*, **16**, 2945–2954.
32. Toffano-Nioche,C., Nguyen,A.N., Kuchly,C., Ott,A., Gautheret,D., Bouloc,P. and Jacq,A. (2012) Transcriptomic profiling of the oyster pathogen *Vibrio splendidus* opens a window on the evolutionary dynamics of the small RNA repertoire in the Vibrio genus. *RNA*, **18**, 2201–2219.
33. Langmead,B. and Salzberg,S.L. (2012) Fast gapped-read alignment with Bowtie 2. *Nat. Methods*, **9**, 357–359.
34. Rutherford,K., Parkhill,J., Crook,J., Horsnell,T., Rice,P., Rajandream,M.A. and Barrell,B. (2000) Artemis: sequence visualization and annotation. *Bioinformatics*, **16**, 944–945.
35. Liao,Y., Smyth,G.K. and Shi,W. (2014) featureCounts: an efficient general purpose program for assigning sequence reads to genomic features. *Bioinformatics*, **30**, 923–930.
36. Varet,H., Brillet-Gueguen,L., Coppee,J.Y. and Dillies,M.A. (2016) SARTools: A DESeq2- and EdgeR-Based R Pipeline for Comprehensive Differential Analysis of RNA-Seq Data. *PLoS One*, **11**, e0157022.
37. Love,M.I., Huber,W. and Anders,S. (2014) Moderated estimation of fold change and dispersion for RNA-seq data with DESeq2. *Genome Biol.*, **15**, 550.
38. Busch,A., Richter,A.S. and Backofen,R. (2008) IntaRNA: efficient prediction of bacterial sRNA targets incorporating target site accessibility and seed regions. *Bioinformatics*, **24**, 2849–2856.
39. Bailey,T.L., Boden,M., Buske,F.A., Frith,M., Grant,C.E., Clementi,L., Ren,J., Li,W.W. and Noble,W.S. (2009) MEME SUITE: tools for motif discovery and searching. *Nucleic Acids Res.*, **37**, W202–W208.
40. Bury-Mone,S., Nomane,Y., Reymond,N., Barbet,R., Jacquet,E., Imbeaud,S., Jacq,A. and Bouloc,P. (2009) Global analysis of extracytoplasmic stress signaling in *Escherichia coli*. *PLos Genet.*, **5**, e1000651.
41. Sambrook,J. and Russell,D. (2001) *Molecular Cloning: a laboratory manual*. 3th edn. Cold Spring Harbor Laboratory Press, NY.
42. Douchin,V., Bohn,C. and Bouloc,P. (2006) Down-regulation of porins by a small RNA bypasses the essentiality of the regulated intramembrane proteolysis protease RseP in *Escherichia coli*. *J. Biol. Chem.*, **281**, 12253–12259.
43. Marchais,A., Naville,M., Bohn,C., Bouloc,P. and Gautheret,D. (2009) Single-pass classification of all noncoding sequences in a bacterial genome using phylogenetic profiles. *Genome Res.*, **19**, 1084–1092.
44. Horsburgh,M.J., Clements,M.O., Crossley,H., Ingham,E. and Foster,S.J. (2001) PerR controls oxidative stress resistance and iron storage proteins and is required for virulence in *Staphylococcus aureus*. *Infect. Immun.*, **69**, 3744–3754.
45. VanDrisse,C.M., Hentchel,K.L. and Escalante-Semerena,J.C. (2016) Phosphinothricin acetyltransferases identified using in vivo, in itro, and bioinformatic analyses. *Appl. Environ. Microbiol.*, **82**, 7041–7051.
46. Geisinger,E., Adhikari,R.P., Jin,R., Ross,H.F. and Novick,R.P. (2006) Inhibition of rot translation by RNAIII, a key feature of *agr* function. *Mol. Microbiol.*, **61**, 1038–1048.
47. Marincola,G., Schafer,T., Behler,J., Bernhardt,J., Ohlsen,K., Goerke,C. and Wolz,C. (2012) RNase Y of *Staphylococcus aureus* and its role in the activation of virulence genes. *Mol. Microbiol.*, **85**, 817–832.
48. Lioliou,E., Sharma,C.M., Caldelari,I., Helfer,A.C., Fechter,P., Vandenesch,F., Vogel,J. and Romby,P. (2012) Global regulatory functions of the *Staphylococcus aureus* endoribonuclease III in gene expression. *PLos Genet.*, **8**, e1002782.
49. Throup,J.P., Zappacosta,F., Lunsford,R.D., Annan,R.S., Carr,S.A., Lonsdale,J.T., Bryant,A.P., McDevitt,D., Rosenberg,M. and Burnham,M.K. (2001) The *srhSR* gene pair from *Staphylococcus aureus*: genomic and proteomic approaches to the identification and characterization of gene function. *Biochemistry*, **40**, 10392–10401.
50. Kinkel,T.L., Roux,C.M., Dunman,P.M. and Fang,F.C. (2013) The *Staphylococcus aureus* SrrAB two-component system promotes resistance to nitrosative stress and hypoxia. *mBio*, **4**, e00696-13.
51. Wilde,A.D., Snyder,D.J., Putnam,N.E., Valentino,M.D., Hammer,N.D., Lonergan,Z.R., Hinger,S.A., Aysanoa,E.E., Blanchard,C., Dunman,P.M. *et al.* (2015) Bacterial hypoxic responses revealed as critical determinants of the host-*Staphylococcus aureus* pathogen outcome by TnSeq analysis of invasive infection. *PLoS Pathog.*, **11**, e1005341.
52. Nuxoll,A.S., Halouska,S.M., Sadykov,M.R., Hanke,M.L., Bayles,K.W., Kielian,T., Powers,R. and Fey,P.D. (2012) CcpA regulates arginine biosynthesis in *Staphylococcus aureus* through repression of proline catabolism. *PLoS Pathog.*, **8**, e1003033.
53. Li,C., Sun,F., Cho,H., Yelavarthi,V., Sohn,C., He,C., Schneewind,O. and Bae,T. (2010) CcpA mediates proline auxotrophy and is required for *Staphylococcus aureus* pathogenesis. *J. Bacteriol.*, **192**, 3883–3892.

54. Gorke,B. and Stulke,J. (2008) Carbon catabolite repression in bacteria: many ways to make the most out of nutrients. *Nat. Rev. Microbiol.*, **6**, 613–624.
55. Marchais,A., Bohn,C., Bouloc,P. and Gautheret,D. (2010) RsaOG, a new staphylococcal family of highly transcribed non-coding RNA. *RNA Biol.*, **7**, 116–119.
56. Mader,U., Nicolas,P., Depke,M., Pane-Farre,J., Debarbouille,M., van der Kooi-Pol,M.M., Guerin,C., Derozier,S., Hiron,A., Jarmer,H. *et al.* (2016) *Staphylococcus aureus* Transcriptome Architecture: From Laboratory to Infection-Mimicking Conditions. *PLos Genet.*, **12**, e1005962.
57. Figueroa-Bossi,N., Valentini,M., Malleret,L., Fiorini,F. and Bossi,L. (2009) Caught at its own game: regulatory small RNA inactivated by an inducible transcript mimicking its target. *Genes Dev.*, **23**, 2004–2015.
58. Eggenhofer,F., Tafer,H., Stadler,P.F. and Hofacker,I.L. (2011) RNApredator: fast accessibility-based prediction of sRNA targets. *Nucleic Acids Res.*, **39**, W149–W154.
59. Gardan,R., Rapoport,G. and Debarbouille,M. (1997) Role of the transcriptional activator RocR in the arginine-degradation pathway of Bacillus subtilis. *Mol. Microbiol.*, **24**, 825–837.
60. Burge,S.W., Daub,J., Eberhardt,R., Tate,J., Barquist,L., Nawrocki,E.P., Eddy,S.R., Gardner,P.P. and Bateman,A. (2013) Rfam 11.0: 10 years of RNA families. *Nucleic Acids Res.*, **41**, D226–D232.
61. Darty,K., Denise,A. and Ponty,Y. (2009) VARNA: Interactive drawing and editing of the RNA secondary structure. *Bioinformatics*, **25**, 1974–1975.